Bio-filler from waste shellfish shell: Preparation, characterization, and its effect on the mechanical properties on polypropylene composites

Hai-Yan Li[a], Ye-Qiang Tan[b], Lu Zhang[a], Yun-Xiang Zhang[b], Yi-Hu Song[b], Ying Ye[a], Mei-Sheng Xia[a,*]

[a] Department of Ocean Science and Engineering, Zhejiang University, Hangzhou 310058, People's Republic of China
[b] Department of Polymer Science and Engineering, Zhejiang University, Hangzhou 310027, People's Republic of China

ABSTRACT

Waste shellfish shell stacking with a significant odor and toxicity which are hazardous to human constitutes a serious environmental hazard. For utilization of waste shellfish shell resource, granule of shellfish shell (SS) was prepared from waste shellfish shell by removing cuticle, crushing, grinding and shearing emulsification and was introduced as a filler to reinforce polypropylene (PP). The mechanical behavior of PP/SS composite shows a higher yield strain, yield strength, tensile strength and elongation at break than traditional commercial calcium carbonate (CC) filled PP. Yield strength of PP/SS composite with 2% SS is improved by 11.1% due to the formation of β-crystalline PP phase. Using waste SS for producing bio-filler for filling PP is an effective and prospective measure to deal with waste SS, which is valuable for industrial production and practical application as fillers for reinforcing polymers.

© 2012 Elsevier B.V. All rights reserved.

1. Introduction

Shellfish shell (SS) is a shellfish aquaculture by-product that has been listed worldwide as one of the worst environmental problems, as it is difficult to dispose the shellfish shells. It reduces the liming value and renders the waste difficult to recycle to land. The SS contains about 95% calcium carbonate (CC) in the form of aragonite and calcite and 5% organic materials such as glycoproteins, polysaccharides, glycosaminoglycan, chitin and other proteins [1,2]. On one hand, at normal temperature, microbial decomposition of the organic matter produces NH_3, H_2S and harmful hydrocarbon gases with a significant odor and toxicity which are hazardous to human; on the other hand, discarded shellfish shell stacking is the breeding places of mosquitoes, flies, mice and insects because the waste SS stacking place with its leachate and moisture is the location of adult mosquito for spawning and larvae breeding habitat. Thus, finding solutions to the problem of SS waste would be a step towards to reduce the environmental problems. It is especially in those countries where the shellfish product industry is well developed. In the China alone, about 10 million tons of this material is disposed in landfills per year [3].

Due to the high cost of the petroleum-derived products or to environmental hazard, a growing effort has emerged in recent years on the research, development, and application of biocomposites [4].

A biocomposite contains at least one constituent that is derived from renewable resources [4], such as CC from *mytilus edulis* shell, *scallop* shell and *pearl oyster* shell [4].

Nacre is one kind of typical biomineral deposited in the inner layer of the shell by many mollusks [5]. It is comprised of stacked platelets ($\sim$0.5 μm thick and $\sim$10 μm wide), arranged in a "brick-and-mortar" microstructure with an organic matrix (20–50 nm thick) interlayer that is traditionally considered as serving as glue between the single platelets. Amongst all the structures found in shells, nacreous structures appear to be the strongest. Currey [5] concluded that the fracture strength in bending varied between 56 and 116 MPa. Jackson et al. [6] studied nacre from the shell of a bivalve mollusk, Pinctada and reported a Young's modulus of approximately 70 GPa for dry and 60 GPa for wet samples, a tensile strength of 170 MPa for dry and 140 MPa for wet samples and a work of fracture varied from 350 to 1240 J/m^3. In contrast, monolithic CC showed a work-of-fracture approximately 3000 times less than that of the composite nacre material [5].

Although there have been several attempts to use SS components for different applications main in the experimental stage with a small amount of demand [7–16], its chemical composition and availability makes it be a potential source of filler for polymers. Now except accumulating on the ground largely, the waste shell is mainly used as calcium feed supplements after grinding directly with price at about 50 dollars per ton in market in China. The composed of approximately 5% organic materials makes it more easily homogeneous dispersed in to organic polymer than inorganic mineral carbon calcium because of the "like dissolve like" rule. The

* Corresponding author. Fax: +86 571 88208891.
 E-mail addresses: rclihaiyan@gmail.com, rclihaiyan@yahoo.com.cn (M.-S. Xia).

main advantages of using SS aragonite as filler are cost reduction and modulus improvement, without drastically increasing the specific gravity of the composite when compare with the normally using inorganic fillers such as mineral SS and talc [17–20]. These characteristics qualify SS as a good candidate for bulk quantity, inexpensive and low load-bearing composite applications, such as the automotive industry, trucks, offices, homes, and factories.

In this article, we demonstrate the ability of granule SS as an alternative filler for polypropylene (PP) by comparing the filler effects of SS and CC on mechanical properties of filled PP and the crystalline structure of PP in the composites. SS powders prepared from shell of *mytilus edulis* which is one kind of a large number of shellfish breeding in China. Removing cuticle and partial easy to be decomposed organic matter by soaking in sodium hydroxide solution for avoiding organic matter inner SS particles decomposition during the plastics processing at about 200 °C. Crushing, grinding and shearing emulsification methods are used for refinement. Particle size analyzer, XRD, SEM, FT-IR, TGA are used for analysis of the size distribution, composition, organic and mineral phases, micro-morphology and thermal stability of SS particles, respectively. It's also an exploratory study of solving the environmental problems caused by waste shell accumulation, providing a new kind of filler to PP and promoting shellfish aquaculture development environment-friendly.

2. Materials and methods

2.1. Materials

Mytilus edulis shell was obtained from Zhoushan Seafood Processing Factory, China. The commercial CC particles (HD55A, 40–500 nm) were purchased from Hengda Industrial Tech. Group Ltd., China. Polypropylene (PP) (PPH-TO3, T30S) with a bulk density 1.04 g/cm^3 and melt index 1.5 g at 230 °C and 2.16 kg was provided by Petroleum & Chem. Co. Ltd., Zhenhai Refining & Chem. Branch, China. Sodium hydroxide, Irganox 1010 and Hydrogen peroxide (30%) were supplied by National Pharmaceutical Group Chem. Reagent Co. Ltd., China.

2.2. Preparation of SS aragonite particles

An improved method for preparation of SS aragonite particles based on the method of Wheeler et al. [21] as follow. A certain amount of *mytilus edulis* shells were washed for removing residual meat, attachments, etc., and were coarsely grinded. The coarsely grinded *mytilus edulis* shells were immersed into 4% sodium hydroxide solution for 48 h for removing the stratum corneum and separating the prismatic layer by ultrasonic for obtaining the nacreous layer by filtrating. The obtained nacreous layer was dried at 100 °C and was roughly grinded using high-speed Chinese medicine grinder for 10 min and subsequently grinded using an AX-4 stirring ball mill (using zirconia balls as grinding media) at a ball-to-powder mass ratio of 6:1 and a rotational speed of 40 rpm for 8 h, yielding the crude SS aragonite powder. The crude SS shell aragonite powder was dispersed into distilled water of 2 L/kg and 30% hydrogen peroxide of 0.25 L/kg and the dispersion was treated using a BME 100 L high shearing mixing emulsifier at a rotational speed 8000 rpm for 8 h. The product was filtrated, dried, and was further scattered again using the AX-4 stirring ball mill for obtaining the SS aragonite particles.

2.3. Preparation of PP composites

An improved method for preparation of PP composites based on the method of Chan et al. [22] and Zuiderduin et al. [23] as follow. Before mixing, PP and SS (or CC) particles were dried in an oven at 100 °C for 2 h. The materials were stored in a desiccator prior to processing. PP and mineral fillers (SS or CC) were mixed with 0.2% (w/w) antioxidant using a Berstorff (ZE 25 × 33D) twin screw extruder with barrel temperatures set at 195/210/200/200/200/200/200 °C at a screw speed of 75 rpm. The extrudents were pelletized. A vertical injection-moulding machine (Morgan Press) was used for preparing tensile samples (ASTM-D638, type IV) for mechanical tests. Prior to mechanical testing, the tensile bars were conditioned at the temperature of 23 ± 2 °C and the relative humidity of 50 ± 5% for 40 h.

2.4. Characterizations

The characterization methods based on the reference of Chan et al. [22] and Zuiderduin et al. [23]. The particle size distribution was determined using a Beckman LS13320 laser particle size analyzer. The composition was identified by the Japanese Rigaku D/max-II B X-ray diffractometer (tube voltage was 40 kV, tube current was 34 mA, Cu target) using Ni-filtered Cu Kα radiation with λ = 0.154068 nm. Infrared spectra were measured using Nexus 670 Fourier Transform Infrared Spectroscopy Instrumentation by KBr pellet pressing method. The micro-morphology was observed using Hitachi S-4800 Field Emission Scanning Electron Microscope at a voltage of 5 kV. Thermogravimetric analyses (TGA) from 0 °C to 1000 °C were performed on a ZRY-2P thermogravimetric analyze at a heating rate of 10 °C/min in nitrogen atmosphere.

Mechanical test as carried out using specimens of 1.5 mm thick, 12 mm wide, and 120 mm long according to ASTM standard method D638 at a cross-head speed of 50 mm/min at 23 °C and 32% relative humidity. Five specimens of each sample were tested and the mean values and standard deviations were calculated. The Hitachi S-4800 Field Emission Scanning Electron Microscope was used to observe the fracture surfaces of tensile tested at 20 kV and photomicrographs were captured for microstructural analysis.

The crystalline structure of PP in the composites was observed using a polarizing microscope. Proper quantities of composites was placed on a slide, heated to 220 °C, transferred in an oven at 150 °C for thermal treatment for 2 h, and subsequently cooled naturally in the oven. The polarizing microscope equipped with crossed polars and a CCD camera was used for morphological observation.

Crystallinity of PP in the composites was examined using a TA Q100 differential scanning calorimetry (DSC) calibrated with indium. A small amount of sample (approximately 10 mg) was placed in an aluminum pan, crimp-sealed and loaded into the DSC chamber purged with nitrogen. The test was carried out in three steps. The first heating step from 30 °C to 210 °C at 10 °C/min was performed to remove any thermal history of the composite and was excluded from any analysis. The sample was then held isothermally at 210 °C for 5 min. The second step involved cooling the sample from 210 °C to 30 °C at 10 °C/min. After the second step, the sample was again held isothermally at 30 °C for 5 min. The third step involving heating from 30 °C to 210 °C at 10 °C/min was then performed. Crystallization and melting were analyzed based on the second and the third steps.

3. Results and discussions

3.1. Characterization of SS powder

3.1.1. X-ray diffraction (XRD)

SS powders were characterized using XRD as shown in Fig. 1(b). The peak positions of XRD patterns are mainly located in the angle range of 26–50° and coincident with those of the standard powder sample of aragonite (CaCO$_3$, JCPDS Card No. 05-0453) and calcite (CaCO$_3$, JCPDS Card No. 05-0586). Intensity of diffraction peaks
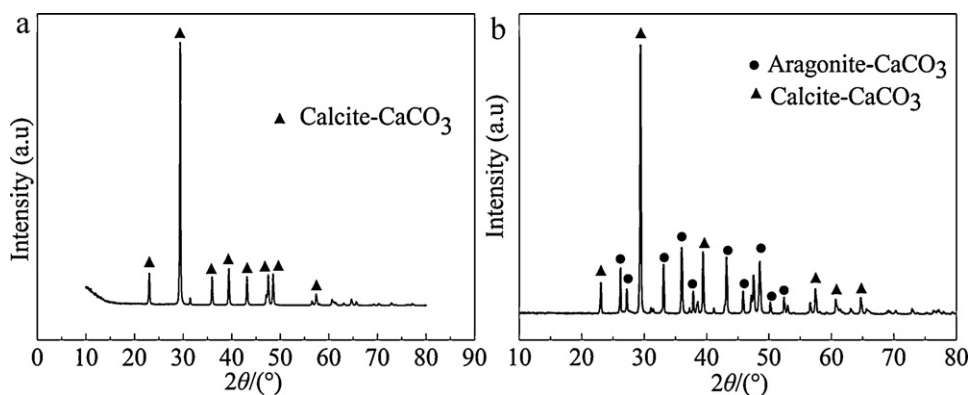
Fig. 1. The XRD pattern of commercial CaCO₃ (a) and shellfish shell powder (b).

of same crystalline planes is obviously different from commercial CaCO₃ as showing in Fig. 1(a). The inorganic in SS powder is mainly aragonite crystal, but SS also contains some calcite crystals too as showing in Fig. 1(b). Some of the calcite crystal may be transferred from the aragonite crystal during the grinding processing. The size of some of SS powders is larger than the thickness of aragonite tablet in nacre. It is reasonable that a part of SS particles are composed of some unbroken aragonite tablets with preferred orientations weaker than in un-grinded nacre.

Nacre located in the inner layer of *mytilus edulis* shell is in a kind of metastable aragonite structure. Stable calcite exists in the outer layer. This kind of structure for the *mytilus edulis* shell can not only reduce the formation energy of shells effectively, but also keep the stability of shells in the natural environment. The inner aragonite layer with regular structure plays an important role for the macroscopic properties of shells [2,13,24–27].

3.1.2. Scanning electron microscope (SEM)

Nacre as a kind of typical biomineral deposited in the inner layer of the shell by many mollusks [1] has been widely studied as a model for understanding biomineralization process and mechanical properties due to the simplicity of its microstructure, in which the aragonite nacre tablets and thin organic sheets are

alternatively arranged like brick-mortar architecture as shows in Figs. 2(a) and (b). As a matter of fact, similar laminated structure has been reported in nacre of seawater bivalve Pinctada shell [28]. The morphology of SS powder with a size distribution ranged from 40 nm to 500 nm is flaky in Fig. 2(c) and (d).

3.1.3. Fourier transform infra-red spectroscopy (FT-IR)

FT-IR spectra of SS are presented in Fig. 3(b), showing the same characteristic bands as natural aragonite. The carbonate group is demonstrated by the vibration modes at 712 (ν_4), 860 (ν_2), 1082 (ν_1) and 1446 (ν_3) cm⁻¹, where ν_3 is the asymmetric stretch, ν_2 is the out-of plane bend and ν_4 is the in-plane bend vibration modes for CO_3^{2-} groups, respectively [29,30]. The strong FT-IR band at 1787 cm⁻¹ could be attributed to the C=O bond of the carbonate groups. The splitting of ν_4 is a characteristic of aragonite structure. The strongest absorption band in the ν_3 region is overlapped by the absorption of the organic component is obviously different from commercial CaCO₃ as showing in Fig. 3(a), revealing the SS powders are composed of both organic and mineral phases. This is corroborated by the FT-IR spectra of material decalcified by EDTA, which had very intense absorption bands in the range 1660–1100 cm⁻¹ [11]. A broad absorption around 3400 cm⁻¹ is due to the stretching vibration of structural water molecules [30].
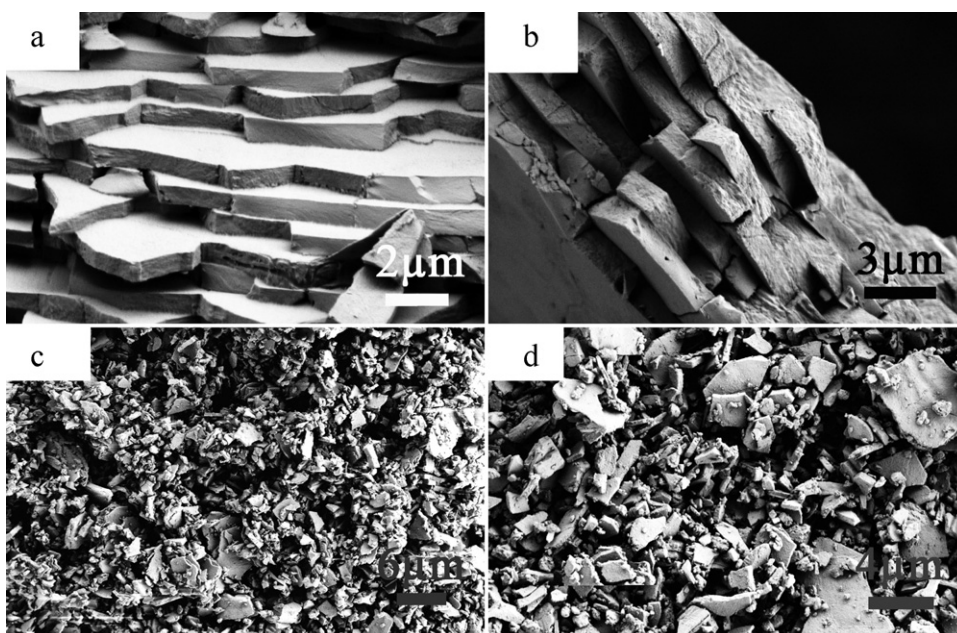

Fig. 2. SEM micrographs of *mytilus edulis* shell: (a) and (b) the cross section of the shellfish shell, and (c) and (d) the shellfish shell powder.
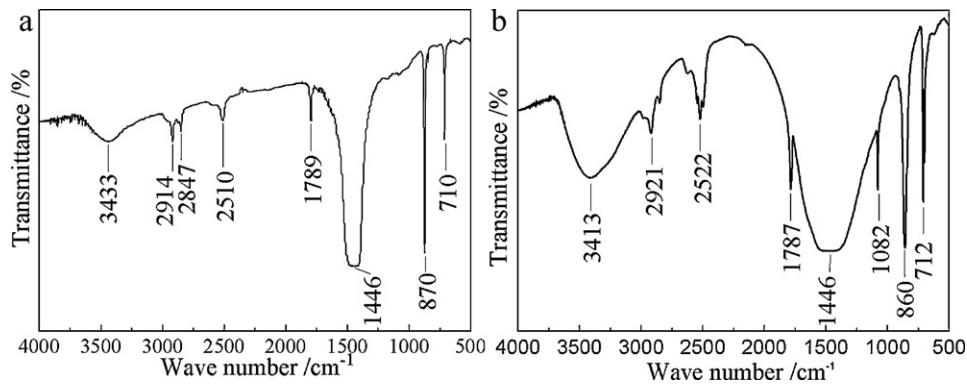
Fig. 3. The Infrared spectroscopy of commercial CaCO$_3$ (a) and shellfish shell powder (b).

3.1.4. TGA

The regularity of microstructure evolution for SS has been investigated by means of analysis of the thermogravimetric-differential thermal curves in Fig. 4. The TGA curve exhibits a moderate intensity exothermic peak at about 262 °C and a weak exothermic peak at 430 °C, which are related to the conversion from aragonite to calcite crystals and the thermal degradation of organism [31]. The strong endothermic peak at about 748 °C is resulted from splitting up of CC in calcite. The transformation temperature of aragonite (390–440 °C) in nacre is lower than that of the natural aragonite at about 450–500 °C [32], which is probably due to the influence of organic component [31]. Because of the strong interaction between the organic and the mineral phases, a part of organic component is destroyed only at around 550–600 °C where the mineral is transformed to calcium oxide. Due to the great thermal stability of the organic component and the organic–mineral bonding [11], the nacreous organic component is strongly linked to the mineral and has a much greater thermal stability than the organic matrix of bone, which may be hopeful for the future use of nacre as a biomaterial for surgical bone repair [11]. Because of the great thermal stability of the organic component, SS powder can be used as a kind of biofiller to blend with PP at about 200 °C.

The loss of weight of SS powder heated from 100 °C to 900 °C is shown in Fig. 4. The loss is quite smaller (about 2.68 wt%) up to 500 °C, while the loss from 700 to 900 °C is about 42.92%. The content of organic component is estimated as 2.68% of the total weight. The overall weight of organic component does not disappear completely, so the organic component should be slightly higher than 2.68%. The weight loss of about 42.92% is caused by CC decomposition.

3.1.5. Size distribution analysis

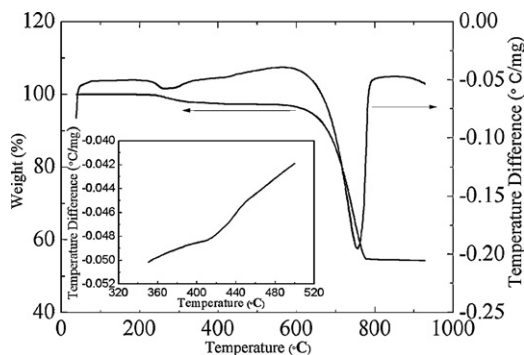Fig. 5 shows size distribution and the corresponding cumulative curve of SS powder. The size distribution is approximate normal with about 60% of the population of grains less than 100 nm and about 90% of the population of grains less than 200 nm in size. The curves also present small regions toward bigger sizes, which could be assigned to particle coalescence.

3.2. Mechanical properties of filled PP

Mechanical properties of PP/SS and PP/CC composites are showed in Fig. 6. The overall characteristic is that the PP/SS composites exhibit mechanical properties superior to the PP/CC composites. Yield strain decreases upon addition of SS and CC particles in Fig. 6(a), which could be related to the debonding of the filler particles from the matrix. However, the PP/SS composites yield at strains higher than the PP/CC composites at the same filler loading, suggesting that the organic matters in the SS powders may bind with the PP matrix more closely. As showed in Fig. 6(b), yield strength of the PP/SS composites is higher than the PP/CC composites at the same filler loading. The PP/SS and the PP/CC composites exhibit maximum yield strength at 3% SS and 1% CC, respectively. Adding CC at high loadings causes yield strength to decrease rapidly while the reduction is rather small in SS filled PP. Filling PP with CC causes a continuous decrease in tension strength and elongation at break reaches a value about 40% strain almost independent of CC content. Filling PP with SS causes tensile strength to decrease from 38 MPa to 33 MPa independent of SS content. Simultaneously, SS filling causes a gradually reduction in elongation at break. As showed in Fig. 6(e), filling causes an increase in Young's modulus. SS filling causes a continuous increase in Young's modulus while the PP/CC composites show a maximum modulus at 5% CC loading, with the improvement of the additive proportion of SS and CC particles.

CC used is one kind of organic modified calcite calcium carbonate while SS is a kind of natural bio-aragonite calcium carbonate containing a small amount of organic matter not only on the surface but also inner between the aragonite tablets. It is expected that the compatibility between SS and PP is better than that between
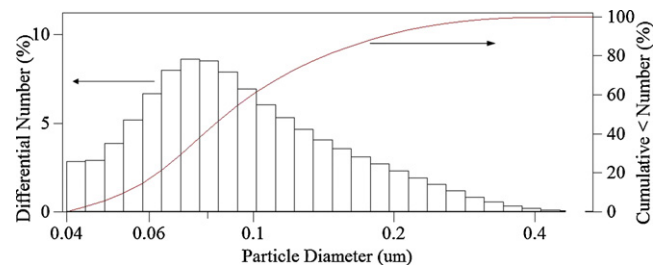

Fig. 4. TGA of shellfish shell powder.

Fig. 5. The particle size distribution of shellfish shell powder.
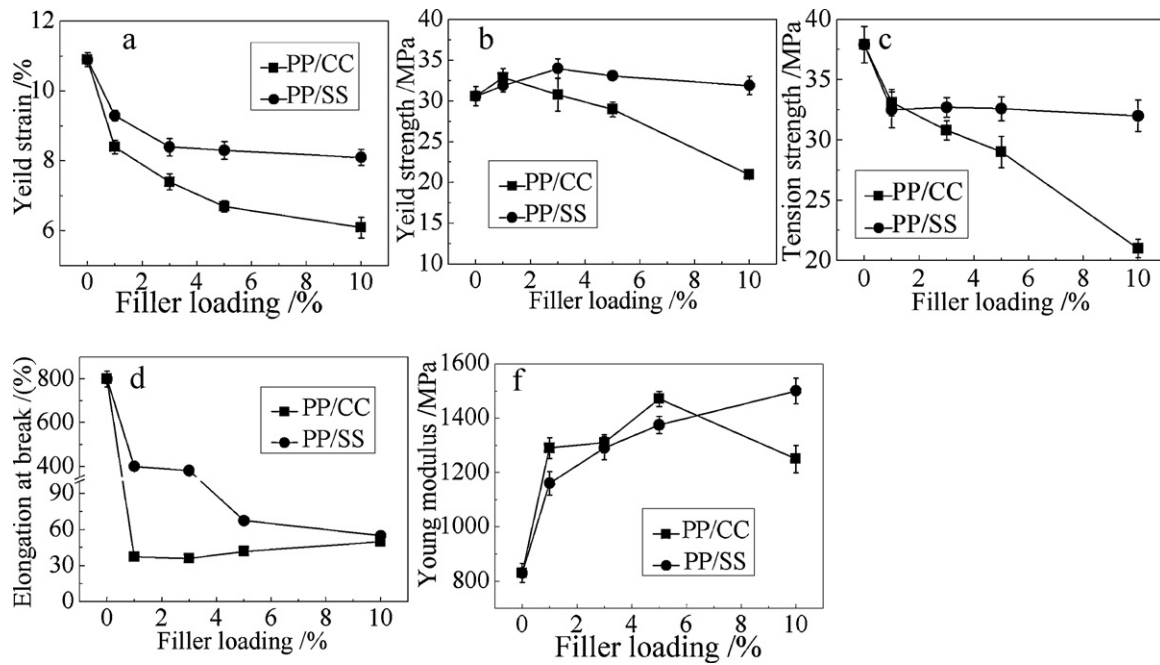
Fig. 6. (a) Yield strain, (b) yield strength, (c) tensile strength, (d) elongation at break and (e) Young's modulus of PP/SS and PP/CC composites.

CC and PP, which explains reinforcement effect of SS superior to than CC. Dispersion of filler in the polymer matrix has a significant effect on the mechanical properties of the composites. It is difficult to achieve a good dispersion of surface modified CC particles in PP by appropriate processing conditions, as shown in Fig. 7 for morphology of the composite with 5% CC. On the other hand, 5% SS particles are finely dispersed in the matrix. Obviously, the organic matter in the SS particles improves the compatibility between PP and SS powders, which is reason for the filling effect of SS superior to CC [24,27,33].

3.3. Effects of SS particles on crystallization and melting behavior of PP

Fig. 8 shows polarized light microscopy (PLM) micrographs of pure PP and the PP/SS composites. Pure PP predominantly consists of α-spherulites with black cross pattern of extinction in Fig. 8(a). With increasing SS content, the black cross pattern of extinction of the PP/SS composites becomes less distinct and the spherulite size decreases, as shown in Fig. 8(b)–(e). The results show that SS can promote the heterogeneous nucleation of PP matrix.
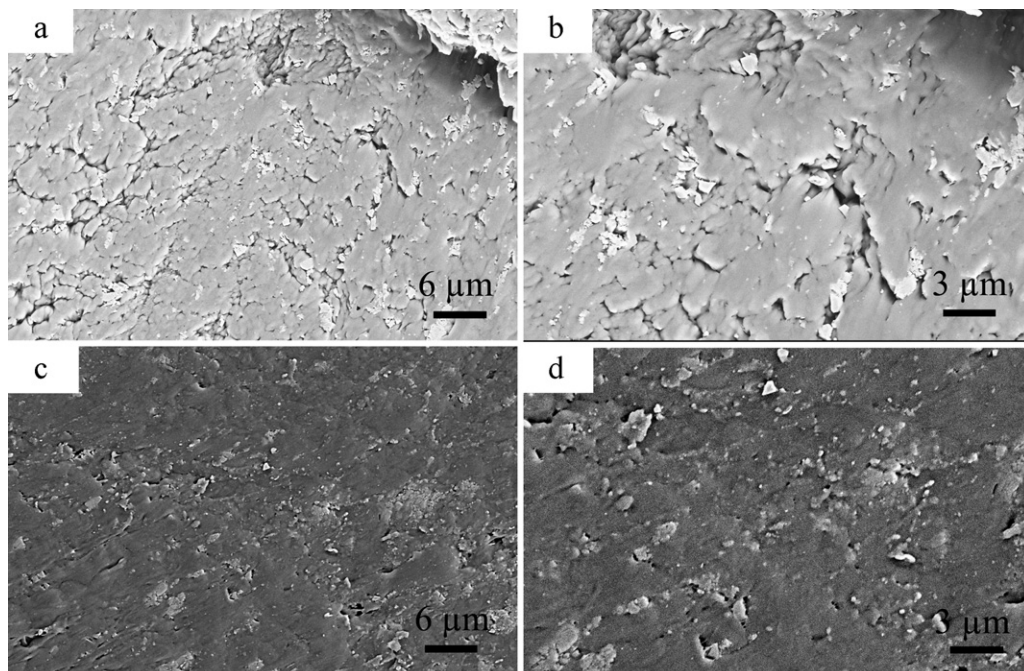

Fig. 7. SEM micrograph of PP/SS (a and b) and PP/CC composites (c and d) containing 5% filler.
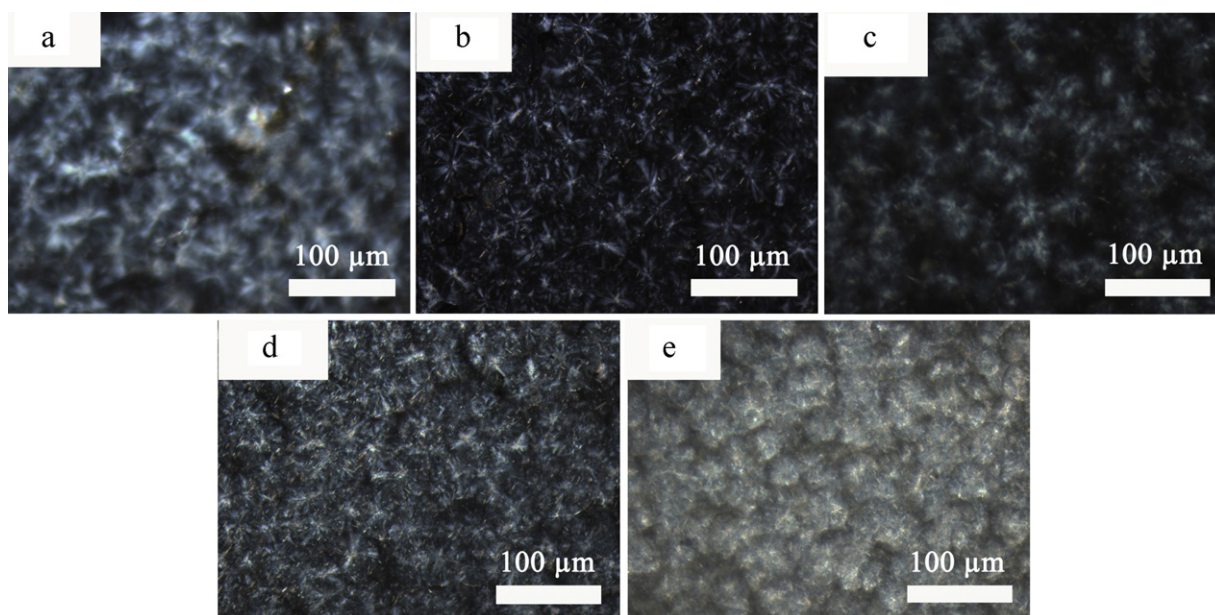
Fig. 8. Polarized light microscope pictures of PP and PP/SS composites (120 °C, 200×): (a) PP, (b) PP + 1% SS, (c) PP + 3% SS, (d) PP + 5% SS, and (e) PP + 10% SS.
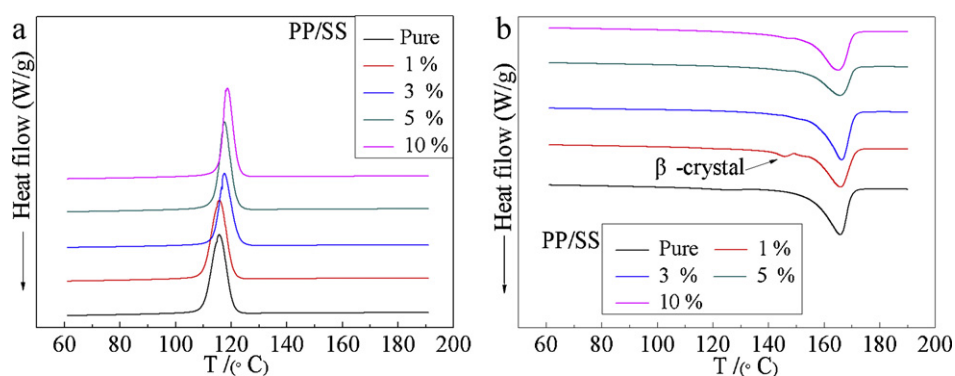

Fig. 9. DSC curves of PP/SS composites at cooling (a) and heating rates of 10 °C/min (b).

DSC thermograms of PP and the PP/SS composites are shown in Fig. 9. With addition of SS powders, the α-PP crystallization peak becomes sharper and the peak temperature moves towards high temperatures, which demonstrates that SS accelerate crystallization of PP. With addition of SS, the melting peak of α-form moves towards low temperatures. At 1% SS, there appears a small melting peak at about 148 °C, which is the sign of the β-PP [34]. At high SS content, the crystal form is still mainly α-form. The formation of β-form crystal is available for adjusting the mechanical properties of filled PP [35].

4. Conclusions

One kind of bio-aragonite of 40–500 nm in size was obtained from *mytilus edulis* shell by removing cuticle, crushing, grinding and shearing emulsification and was used as filler to PP. Mechanical properties of SS filled PP are superior to PP filled with CC. A small content of SS could promote the formation β-crystalline PP. Using shellfish shell for producing bio-aragonite for filling PP can reduce material cost and it is valuable for industrial production and practical application.

Acknowledgements

References

[1] F. Marin, G. Luquet, Molluscan biomineralization: the proteinaceous shell constituents of *Pinna nobilis* L., Mater. Sci. Eng. C 25 (2005) 105–111.
[2] M.A. Meyers, A.Y.M. Lin, P.Y. Chen, J. Muyco, Mechanical strength of abalone nacre: role of the soft organic layer, J. Mech. Behav. Biomed. 1 (2008) 76–85.
[3] National Bureau of Statistics of the People's Republic of China, China Statistical Yearbook 2010, China Statistics Press, Beijing, 2010.
[4] P. Toro, R. Quijada, M. Yazdani-Pedram, J.L. Arias, Eggshell: a new bio-filler for polypropylene composites, Mater. Lett. 61 (2007) 4347–4350.
[5] J.D. Currey, P. Zioupos, D. Peter, A. Casinos, Mechanical properties of nacre and highly mineralized bone, Proc. R. Soc. Lond. B: Biol. Sci. 268 (2001) 107–111.
[6] A. Jackson, J. Vincent, R. Turner, The mechanical design of nacre, Proc. R. Soc. Lond. B: Biol. Sci. 234 (1988) 415–430.
[7] K. Oikawa, T. Asada, K. Yamamoto, H. Wakabayashi, M. Sasaki, M. Sato, J. Matsuda, Antibacterial activity of calcined shell calcium prepared from wild surf clam, J. Health Sci. 46 (2000) 98–103.
[8] H. Gao, H. Chen, W. Chen, F. Tao, Y. Zheng, Y. Jiang, H. Ruan, Effect of nanometer pearl powder on calcium absorption and utilization in rats, Food Chem. 109 (2008) 493–498.

[9] C.H. Lee, D.K. Lee, M.A. Ali, P.J. Kim, Effects of oyster shell on soil chemical and biological properties and cabbage productivity as a liming materials, Waste Manage. 28 (2008) 2702–2708.

[10] T. Takada, A. Furusaki, Y. Tanaka, Formaldehyde reduction with scallop shell powders fired at high temperatures: identification of the effective ingredient, Bio-Med. Mater. Eng. 19 (2009) 187–192.

[11] J. Balmain, B. Hannoyer, E. Lopez, Fourier transform infrared spectroscopy (FTIR) and X-ray diffraction analyses of mineral and organic matrix during heating of mother of pearl (nacre) from the shell of the mollusc *Pinctada maxima*, J. Biomed. Mater. Res. 48 (1999) 749–754.

[12] H.B. Kwon, C.W. Lee, B.S. Jun, J. Yun, S.Y. Weon, B. Koopman, Recycling waste oyster shells for eutrophication control, Resour. Conserv. Recycl. 41 (2004) 75–82.

[13] M. Shono, I. Shimizu, E. Aoyagi, T. Taniguchi, H. Takenaka, M. Ishikawa, M. Urata, K. Sannomiya, K. Tamaki, N. Harada, Reducing effect of feeding powdered nacre of *Pinctada maxima* on the visceral fat of rats, Biosci. Biotechnol. Biochem. 72 (2008) 2761–2763.

[14] W. Mayes, J. Davis, V. Silva, A. Jarvis, Treatment of zinc-rich acid mine water in low residence time bioreactors incorporating waste shells and methanol dosing, J. Hazard. Mater. 193 (2011) 279–287.

[15] C. Li, P. Champagne, Fixed-bed column study for the removal of cadmium(II) and nickel(II) ions from aqueous solutions using peat and mollusk shells, J. Hazard. Mater. 171 (2009) 872–878.

[16] N.A. Oladoja, Y.D. Aliu, Snail shell as coagulant aid in the alum precipitation of malachite green from aqua system, J. Hazard. Mater. 164 (2009) 1496–1502.

[17] P. Etel aho, S. Haveri, P. Jaervelae, Comparison of the morphology and mechanical properties of unmodified and surface-modified nanosized calcium carbonate in a polypropylene matrix, Polym. Compos. 32 (2011) 464–471.

[18] H. Azizi, J. Faghihi, An investigation on the mechanical and dynamic rheological properties of single and hybrid filler/polypropylene composites based on talc and calcium carbonate, Polym. Compos. 30 (2009) 1743–1748.

[19] J. Zhang, B. Han, N.L. Zhou, J. Fang, J. Wu, Z.M. Ma, H. Mo, J. Shen, Preparation and characterization of nano/micro-calcium carbonate particles/polypropylene composites, J. Appl. Polym. Sci. 119 (2011) 3560–3565.

[20] S. Jipa, T. Zaharescu, P. Supaphol, Thermal stability of isotactic polypropylene modified with calcium carbonate nanoparticles, Polym. Bull. 64 (2010) 783–790.

[21] A.P. Wheeler, J.W. George, C.A. Evans, Control of calcium carbonate nucleation and crystal growth by soluble matrix of oyster shell, Science 212 (1981) 1397.

[22] C.M. Chan, J. Wu, J.X. Li, Y.K. Cheung, Polypropylene/calcium carbonate nanocomposites, Polymer 43 (2002) 2981–2992.

[23] W.C.J. Zuiderduin, C. Westzaan, J. Huetink, R.J. Gaymans, Toughening of polypropylene with calcium carbonate particles, Polymer 44 (2003) 261–275.

[24] F. Barthelat, C.M. Li, C. Comi, H.D. Espinosa, Mechanical properties of nacre constituents and their impact on mechanical performance, J. Mater. Res. 21 (2006) 1977–1986.

[25] L. Xie, X.X. Wang, J. Li, The SEM and TEM study on the laminated structure of individual aragonitic nacre tablet in freshwater bivalve *H. cumingii* Lea shell, J. Struct. Biol. 169 (2010) 89–94.

[26] F. Ren, X. Wan, Z. Ma, J. Su, Study on microstructure and thermodynamics of nacre in mussel shell, Mater. Chem. Phys. 114 (2007) 367–370.

[27] K.S. Katti, D.R. Katti, Why is nacre so tough and strong? Mater. Sci. Eng. C 26 (2006) 1317–1324.

[28] D. Jacob, A. Soldati, R. Wirth, J. Huth, U. Wehrmeister, W. Hofmeister, Nanostructure, composition and mechanisms of bivalve shell growth, Geochim. Cosmochim. Acta 72 (2008) 5401–5415.

[29] K. Naemchanthara, S. Meejoo, W. Onreabroy, P. Limsuwan, Temperature effect on chicken egg shell investigated by XRD, TGA and FTIR, Adv. Mater. Res. 55 (2008) 333–336.

[30] B. Engin, H. Demirtas, M. Eken, Temperature effects on egg shells investigated by XRD, IR and ESR techniques, Radiat. Phys. Chem. 75 (2006) 268–277.

[31] F.Z. Ren, X.D. Wan, P. Liu, G. Jia, S.B.H. Tian, Microstructure and infra-red spectra analysis of mussel shell, J. Henan Univ. S&T (Nat. Sci.) 28 (2007) 1–4.

[32] A. Baumer, M. Ganteaume, M. Bernat, Included water in corals for the transition aragonite to calcite, Thermochim. Acta 221 (1993) 255–262.

[33] P.Y. Chen, A. Lin, Y.S. Lin, Y. Seki, A. Stokes, J. Peyras, E. Olevsky, M. Meyers, J. McKittrick, Structure and mechanical properties of selected biological materials, J. Mech. Behav. Biomed. 1 (2008) 208–226.

[34] M.R. Meng, Q. Dou, Effect of filler treatment on crystallization, morphology and mechanical properties of polypropylene/calcium carbonate composites, J. Macromol. Sci. Phys. 48 (2009) 213–225.

[35] J. Kotek, I. Kelnar, J. Baldrian, M. Raab, Tensile behaviour of isotactic polypropylene modified by specific nucleation and active fillers, Eur. Polym. J. 40 (2004) 679–684.